PROGRESS IN TIME-RESOLVED MeV TRANSMISSION ELECTRON MICROSCOPY AT UCLA[*]

P. Denham[†], N. Burger D. Cesar, D. Dang, P. Musumeci,
University of California Los Angeles, Los Angeles, CA, USA

Abstract

We present current progress on the implementation of two new enhancements developed for the time-resolved relativistic electron microscope at the UCLA PEGASUS Lab based on the use of a radiofrequency photoinjector as an ultrafast electron source and permanent magnet quadrupoles as electron lenses. The first enhancement is a flexible optical column design which would add the capability to switch between imaging the sample and its diffraction pattern, and a collimator to improve imaging contrast. The second enhancement is a high-frequency (X-band) cavity downstream from the (S-band) photoinjector to reduce the beam energy spread. These additions are crucial for improving contrast and image quality. Furthermore, a pulse-wire alignment method is used to fiducialize the quadrupole positions to (better than 20-um precision) to reduce the aberrations induced by misalignment and achieve spatial resolution at the 20 nm-level.

INTRODUCTION

Time-resolved electron microscopes capable of delivering single-shot real-space images with a spatial/temporal resolutions of 10 nm/10 ps are highly desired scientific tools in the material science community [1]. For example, in the study of defect/dislocation motion. In order to reach these levels of spatio-temporal resolutions, relativistic electron energies are required to suppress the space charge effects which would otherwise limit the performance of the instrument. A recently discussed concept for MeV electron microscopy [2] relies on high gradient quadrupole triplet lenses compatible with the higher energies and compact space, and radiofrequency technology to quickly accelerate, ballistically bunch, reduce the energy spread of, or streak the electron beam [3]. By utilizing RF-technology and advancements in pulsed laser systems, a variety of imaging modalities can be exploited as for example a double exposure electron column [4] intended for studying irreversible processes just before and right after they happen.

The Pegasus single-shot picosecond TEM (SPTEM) design [2] starts with a high-gradient RF gun operating in the cigar regime in order to optimize transverse beam brightness [3, 5]. A two solenoid condenser then transports and focuses the beam down onto the sample, after which permanent magnet quadrupole (PMQ) triplets [6] form the objective and projector/magnification lenses. In previous work [7, 8], we have demonstrated 40x magnification with the PMQ sys-

tem [6] and demonstrated that they are a viable choice for an MeV microscope.

In this work we consider few improvements to the microscope design: firstly we discuss adding an intermediary lens to the optical column which can be used to image the back focal plane of the objective lens; secondly we consider using an RF cavity to reduce the bunch energy spread; lastly we discuss the pulse wire technique as a method to align each quadruple within the triplet.

FLEXIBLE OPTICAL COLUMN

A crucial requirement of a microscope is the ability to switch between imaging the diffraction pattern and the projected shadow of a sample. In particular, flexible optics with the ability to instantly transition between diffraction and real space imaging must be paired with a collimator to provide a contrast mechanism to distinguish between the unscattered and scattered electrons [7]. Here we show that inserting an electromagnetic (EM) quadrupole triplet in-between the objective and magnification lenses can provide the necessary flexibility. When the EM triplet is off, the sample is imaged onto the detector. When the EM triplet is turned on, the back focal plane (BFP) is imaged. Then a collimator on a actuator will be placed at one of the BFPs of the first triplet (the other BFP is actually inside the triplet). The purpose of this will become clear shortly. The optical layout is shown in Fig. 1.
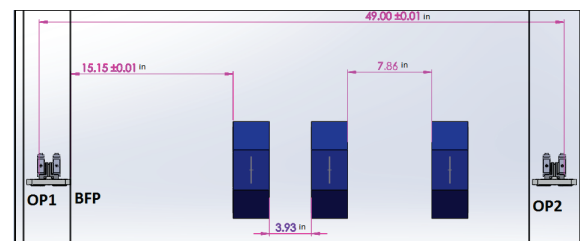

Figure 1: The two object planes of each PMQ triplet are labelled OP1 and OP2 respectively as solid lines. One of the BFPs of the objective lens is indicated as well. The positions are qualitatively placed for perspective. The blue quadrupole triplet is made from electromagnetic quadrupoles which are tuned to image the BFP at OP2.

The currents in the EM triplet are numerically optimized by using a thick lens matrix model of the entire optical setup. For our optimization, the dynamics for each transverse dimension is described by an algebraic system consisting of

the following matrices:

$$R_{quad} = \begin{pmatrix} \cos(\sqrt{k}L) & \frac{1}{\sqrt{k}}\sin(\sqrt{k}L) \\ -\sqrt{k}\sin(\sqrt{k}L) & \cos(\sqrt{k}L) \end{pmatrix} , \quad (1)$$

$$R_{drift} = \begin{pmatrix} 1 & d \\ 0 & 1 \end{pmatrix} , \quad (2)$$

$$(x, x')^T = R(x_0, x_0')^T , \quad (3)$$

where the quadrupole has strength $k = G/B\rho$ and length L, and drift spaces have length d. The gradients switch sign for each quadrupole and for the other dimension, yielding the hyperbolic functions cosh and sinh. The total transport matrix for each transverse dimension is constructed and the gradients are tuned until the appropriate imaging condition is found.

The quadrupole strengths are determined by solving for currents which ensure the 4D transport matrix from the sample to the detector is given by:

$$R_{diff} = \begin{pmatrix} 0 & r & 0 & 0 \\ -1/r & s & 0 & 0 \\ 0 & 0 & 0 & r \\ 0 & 0 & -1/r & t \end{pmatrix} , \quad (4)$$

where r is the angular magnification, and s and t are derivatives of the sine-like principal trajectories at the detector plane [9]. This matrix transformation maps all of the initial coordinates to their initial angles at the detector plane, thus providing the means of fourier transforming the sample image. By moving a collimator and utilizing the aperture of the PMQ triplet, high scattering angle trajectories can be intercepted resulting in contrast at the detector plane. The relevant matrix parameters for the diffraction mode are shown in Fig. 2 . The effective drift length of the diffraction camera, $M_{12} = 0.25$m, implies that a 1 mrad diffraction angle will be spread out to 250μm on the detector screen. This provides sufficient working space to separate the diffraction peaks with a mechanical aperture allowing the microscope operator to optimally place the aperture in the back focal plane of the objective lens.

ENERGY SPREAD COMPENSATION

Relying on diffraction contrast puts a strict requirement on the transverse beam emittance as this quantity determines how well we can distinguish the diffraction spots and enhance the contrast with the collimator. Therefore, we want to use a small spot on the cathode, and to preserve the total charge we plan to employ a relatively long electron beam ($\approx$ 10ps). However, when we use a long electron beam, we are sensitive to the RF field curvature. To compensate for the energy spread, an X-band cavity is placed after the exit of the 1.6 cell gun. The electrons exiting the gun (f=2.856Ghz) within a range a few ps earlier or later than the reference design particle are distributed temporally along a quadratic curve in the longitudinal phase space. The rms energy spread of this distribution before compensation is on the order of
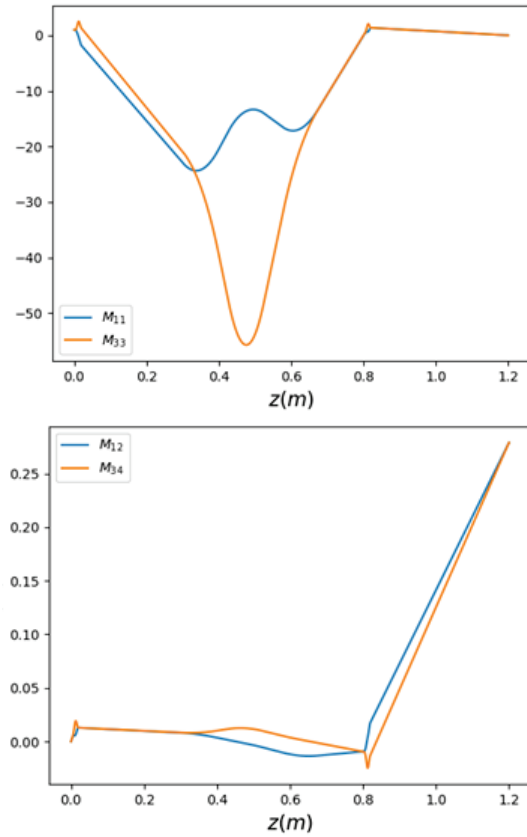
Figure 2: (Top) Both M_{11} and M_{33} are shown at each position along the optical column. These elements are both zero at the final image plane. (Bottom) Correspondingly, M_{12} and M_{34} are equal at the image plane.

10^{-3} [2]. Here we show GPT simulation results that a short x-band cavity (f=9.6Ghz) located after the gun can be used to adequately compensate through second order this RF-induced energy spread. The HFSS model of the X-band is shown in Fig. 3.
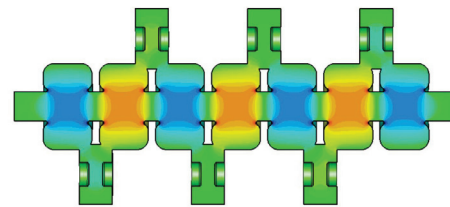

Figure 3: Profile of the X-band Cavity.

We analyzed the longitudinal phase space (LPS) of a 3ps long beam before and after the x-band linearizer is turned on. Optimal compensation parameters for the X-band cavity are found by fitting the longitudinal phase space of the beam to a quadratic expression and then tune the phase and amplitude of the field inside the X-band to minimize the coefficients. The results of the GPT simulations are shown in Fig. 4. The projected rms energy spread of the beam for optimal cavity parameters is below the requirement of 10^{-4} for avoiding
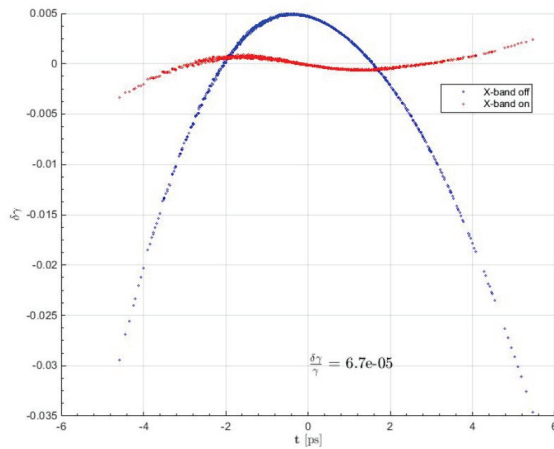
Figure 4: LPS of the beam with x-band cavity off (blue) and on (red). The relative energy spread $\delta\gamma/\gamma$ is reduced to 6.7e-5.

chromatic aberrations [2]. Thus, with the current 1.6 cell photo-injector as the source, and the X-band cavity operating at a peak accelerating voltage of 410kV and a phase of -4 deg, we can obtain a final rms energy spread of $6.7e - 5$.

PULSE WIRE ALIGNMENT

One of the main factors in degrading the microscope resolution is transverse misalignment of PMQs. The current goal is to align the optics to within $20\mu m$ to achieve sub 20nm resolution [8]. The strategy employed to obtain this level of alignment precision is to use a pulsed wire technique. The technique relies on measuring the deflection of a wire strung through the PMQ triplet. The deflection is caused by the PMQ triplet's impulse on the wire in response to a $< \mu s$ applied voltage bias across the wire. The bias duration is selected so the distance the mechanical wave travels in the time of a current pulse is small in comparison to the spacing between PMQ's. When the initial impulse on the wire is assumed to be proportional to a delta function, the wire deflection can be modeled by:

$$x(z,t) = \frac{I_0 x_m \Delta t}{2\rho c} \int_{z-ct}^{z+ct} G(z)dz \qquad (5)$$

Where $G(z)$, x_m, I_0, Δt, ρ and c, are the triplet's gradient profile, initial wire deflection, current in the wire, pulse width, linear mass density, and wave speed respectively [10]. The limits of integration correspond to two waves travelling in opposite directions. The wire displacement signature is a voltage signal from a photo-diode sensitive enough to detect intensity fluctuations. The wire equilibrium is positioned in the laser intensity profile so that the photo-diode signal varies linearly with displacement of the wire. In Fig. 5, measurements of the peak photo-diode signal as the wire is displaced from the magnetic axis are shown. These measurements give a preliminary estimate of what degree of misalignment can be resolved. The rms photo-diode noise is $\approx 0.1mV$ corresponding to a 0.04mm alignment tolerance.
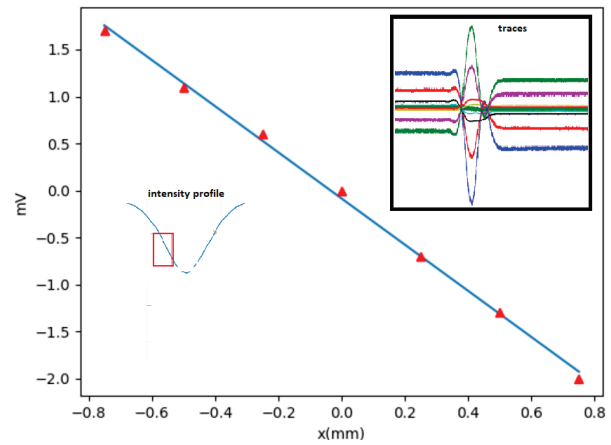

Figure 5: (Top Right) Pulse wire traces as a function of mis-alignment. The steep slopes in each trace corresponds to a PMQ. A perfectly aligned triplet would have $I_0 = 0$, and thus be perfectly flat. The linear plot shows a calibration indicating that 2.2mV corresponds to 1 mm of triplet displacement. The intensity profile and linear region are shown in the lower left.

In Fig. 5, the slope relates this signal to roughly 0.04mm, which is about a factor of 2 larger than the desired level of precision.

CONCLUSION

In this paper, we presented progress on improving the resolution and imaging modalities of a time-resolved TEM driven by an rf photoinjector. A quadrupole-based diffraction imaging system is discussed and analyzed by a transfer matrix description paired with numerical optimizations. This analysis reveals solutions compatible with the compact space requirements of the PEGASUS beamline. The plan is to implement this triplet with a collimator to control the contrast of sample images. Optimized simulations of a high frequency, X-band, rf cavity were presented. The results suggested that a reduction of the relative rms energy spread below 10^{-4} is possible. It is presumed that this level of reduction will suitably minimize the effects of chromatic aberration from the optical column. Finally, a pulse wire method was utilized to improve the alignment of quadrupole triplets used at the PEGASUS beamline to within $20\mu m$. So far, the best we have managed is roughly $40\mu m$.

ACKNOWLEDGEMENTS

REFERENCES

[1] F. Carbone, P. Musumeci, O. Luiten, and C. Hebert, "A perspective on novel sources of ultrashort electron and x-ray pulses," *Chemical Physics*, vol. 392, no. 1, pp. 1 – 9, 2012.

[2] R. K. Li and P. Musumeci, "Single-shot mev transmission electron microscopy with picosecond temporal resolution," *Phys. Rev. Appl.*, vol. 2, p. 024003, Aug 2014.

[3] J. Maxson, D. Cesar, G. Calmasini, A. Ody, P. Musumeci, and D. Alesini, "Direct measurement of sub-10 fs relativistic electron beams with ultralow emittance," *Phys. Rev. Lett.*, vol. 118, p. 154802, Apr 2017.

[4] P. Musumeci, D. Cesar, and J. Maxson, "Double-shot mev electron diffraction and microscopy," *Structural Dynamics*, vol. 4, p. 044025, July 2017.

[5] J. Rosenzweig, A. Cahill, B. Carlsten, G. Castorina, M. Croia, C. Emma, A. Fukusawa, B. Spataro, D. Alesini, V. Dolgashev, M. Ferrario, G. Lawler, R. Li, C. Limborg, J. Maxson, P. Musumeci, R. Pompili, S. Tantawi, and O. Williams, "Ultrahigh brightness electron beams from very-high field cryogenic radiofrequency photocathode sources," 3rd European Advanced Accelerator Concepts workshop (EAAC2017), *Nuclear Instrum. Methods A,* vol. 909, pp. 224–228, 2018.

[6] J. K. Lim, P. Frigola, G. Travish, J. B. Rosenzweig, S. G. Anderson, W. J. Brown, J. S. Jacob, C. L. Robbins, and A. M. Tremaine, "Adjustable, short focal length permanent-magnet quadrupole based electron beam final focus system," *Phys. Rev. ST Accel. Beams*, vol. 8, p. 072401, Jul 2005.

[7] D. B. Cesar, "Probing Ultrafast Dynamics with Relativistic Electrons." Ph.D. thesis, UCLA, 2019.

[8] D. Cesar, J. Maxson, P. Musumeci, Y. Sun, J. Harrison, P. Frigola, F. H. O'Shea, H. To, D. Alesini, and R. K. Li, "Demonstration of single-shot picosecond time-resolved mev electron imaging using a compact permanent magnet quadrupole based lens," *Phys. Rev. Lett.*, vol. 117, p. 024801, Jul 2016.

[9] H. Wiedemann, *Particle Accelerator Physics*, 3rd. Ed., Berlin: Springer, 2007.

[10] R. Warren, "Limitations on the use of the pulsed-wire field measuring technique," *Nuclear Instrum. Methods A*, vol. 272, no. 1, pp. 257–263, 1988.